Hindawi Publishing Corporation
Mathematical Problems in Engineering
Volume 2013, Article ID 463760, 7 pages
http://dx.doi.org/10.1155/2013/463760

Research Article

An Image Filter Based on Multiobjective Genetic Algorithm and Shearlet Transformation

Zhi-yong Fan,[1,2] Quan-sen Sun,[1] Ze-xuan Ji,[1] and Kai Hu[2]

[1] *Nanjing University of Science and Technology, Nanjing 210000, China*
[2] *Nanjing University of Information Science and Technology, Nanjing 210044, China*

Correspondence should be addressed to Quan-sen Sun; quansen179189237@163.com

Received 4 June 2013; Revised 22 July 2013; Accepted 26 August 2013

Academic Editor: Marco Perez-Cisneros

Rician noise pollutes magnetic resonance imaging (MRI) data, making data's postprocessing difficult. In order to remove this noise and avoid loss of details as much as possible, we proposed a filter algorithm using both multiobjective genetic algorithm (MOGA) and Shearlet transformation. Firstly, the multiscale wavelet decomposition is applied to the target image. Secondly, the MOGA target function is constructed by evaluation methods, such as signal-to-noise ratio (SNR) and mean square error (MSE). Thirdly, MOGA is used with optimal coefficients of Shearlet wavelet threshold value in a different scale and a different orientation. Finally, the noise-free image could be obtained through inverse wavelet transform. At the end of the paper, experimental results show that this proposed algorithm eliminates Rician noise more effectively and yields better peak signal-to-noise ratio (PSNR) gains compared with other traditional filters.

1. Introduction

Magnetic resonance imaging (MRI) devices are important imaging equipment, and the image quality directly impacts the diagnosis accuracy. However, MRI images are frequently contaminated by Rician noise during image gaining or transmission [1]. This phenomenon makes noise reduction to be one of the most important problems in image processing. Preservation of image details and attenuation of noise are both critical, but they are contradictory in nature. Therefore, this research is focused on Rician noise elimination and data details preservation at the same time.

Because of its good performance in both time domain and frequency domain, wavelet transform has become one of the most active research fields in image processing. It provides better results and preserves more details compared with traditional algorithms. However, wavelet transform cannot achieve optimal sparse for images containing higher-dimension singularity. To overcome the limitation, multiscale geometric analysis theory is proposed, and, based on it, a series of methods sprang out, for example, ridgelet [2], curvelet [3], contourlet [4], and bandlet [4]. One of the most successful ideas is the curvelets of Candes and Donoho, which achieve an (almost) optimal approximation for 2D piecewise smooth functions with discontinuities along with C^2 curves.

Recently, Labate et al. described a new class of multidimensional representation systems, which is called Shearlet. One advantage of this approach is that these systems can be constructed using generalized multiresolution analysis and implemented efficiently using a classical cascade algorithm [5–11].

Simple threshold denoising method of classical Shearlet transform could yield good performance because of the method's multiscale and multidirection characteristics and image sparse representation. However, there is still room for improvement because classical Shearlet algorithm does not take energy distribution of different scales and different directions into consideration; as a result, it kills the coefficient excessively; therefore, image details could be lost. In order to solve the problem, Sun and Zhao [12] proposed a particle swarm optimization; it uses adaptive algorithm to search for optimal threshold of the highest PSNR values.

Based on these previous achievements, this paper proposed a new image-filtering algorithm. It has three characteristics: it uses soft threshold in Shearlet, it builds target function in MOGA by several evaluation methods, and it

uses the MOGA to optimize coefficients of Shearlet wavelet threshold value in different scale and a different orientation.

The rest of this paper is organized as follows. Section 2 introduces related theories. Section 3 explains our algorithm, including workflow, Section 4 presents the experiment results of proposed algorithm, and Section 5 concludes this paper.

2. Related Theories

2.1. Rician Noise. Noised MRI image v can be defined as $v_{(i)} = u_{(i)} + n_{(i)}$; here, $u_{(i)}$ represent original image pixels, and $n_{(i)}$ represent is noised pixels. When MR images are computed by using the magnitude of single-complex raw data, its distribution can be modeled as a Rician model [13–15]. Consider the following:

$$p(m) = \frac{m}{\sigma_n^2} e^{-(m^2+A^2)/2\sigma_n^2} I_0\left(\frac{Am}{\sigma_n^2}\right). \tag{1}$$

Here, σ^2 is the standard deviation (STD) of Gaussian noise, A is the amplitude of the signal without noise, x is the value of the magnitude image, and I_0 is the 0th-order modified Bessel function. This model is used by the majority of the noise estimation methods.

When SNR is small enough (i.e., SNR = 0), the Rician distribution is considered as a Rayleigh distribution. Consider the following:

$$p(m) = \frac{m}{\sigma_n^2} e\left(\frac{m^2}{\sigma_n^2}\right). \tag{2}$$

When SNR is high (i.e., SNR > 3), the Rician distribution is approximated as a Gaussian distribution.

$$p(m) = \frac{1}{2\pi\sigma^2} e\left(-\frac{\left(m^2 - \sqrt{A^2+\sigma_n^2}\right)^2}{2\sigma_n^2}\right). \tag{3}$$

2.2. Shearlet Transform. Labate et al. [5–11] proposed Shearlet transform based on wavelet. With dimension $n = 2$, consider the following affine system:

$$\Psi_{AB}(\psi) = \left\{\psi_{j,l,k}(x) = |\det A|^{j/2}\psi\left(B^l A^j x - k\right) : j,l \in \mathbb{Z}, k \in \mathbb{Z}^2\right\}. \tag{4}$$

Here, $\psi \in L^2(\mathbb{R}^2)$, and A, B are $2*2$ invertible matrices with $|\det B| = 1$.

If $\Psi_{AB}(\psi)$ satisfied Parseval $L^2(\mathbb{R}^2)$, then, those elements of $\Psi_{AB}(\psi)$ are called composite wavelets.

Shearlet is a special example of $L^2(\mathbb{R}^2)$ only when

$$A = A_0 = \begin{pmatrix} 4 & 0 \\ 0 & 2 \end{pmatrix}, \qquad B = B_0 = \begin{pmatrix} 0 & 1 \\ 1 & 1 \end{pmatrix}. \tag{5}$$

Here, $A = A_0$ is the anisotropic dilation matrix, and $B = B_0$ is the shear matrix.

For $\xi = (\xi_1, \xi_2) \in \widehat{\mathbb{R}}^2$, $\xi_1 \neq 0$, when $\psi^{(0)}$, $\widehat{\psi}_1$, and $\widehat{\psi}_2$ satisfy

$$\begin{aligned} \widehat{\psi}^{(0)}(\xi) = \widehat{\psi}^{(0)}(\xi_1,\xi_2) &= \widehat{\psi}_1(\xi_1)\,\widehat{\psi}_2\left(\frac{\xi_2}{\xi_1}\right), \\ \widehat{\psi}_1, \widehat{\psi}_2 &\in C^\infty\left(\widehat{\mathbb{R}}\right), \\ \operatorname{supp}\widehat{\psi}_1 &\subset \left[-\frac{1}{2}, -\frac{1}{16}\right] \cup \left[\frac{1}{16}, \frac{1}{2}\right], \\ \operatorname{supp}\widehat{\psi}_2 &\subset [-1,1], \\ \sum_{j\geq 0}\left|\widehat{\psi}_1\left(2^{-2j}\omega\right)\right|^2 = 1 \quad &\text{for } |\omega| \geq \frac{1}{8},\ j \geq 0, \\ \sum_{l=-2^j}^{2^j-1}\left|\widehat{\psi}_2\left(2^j\omega - l\right)\right|^2 = 1 \quad &\text{for } |\omega| \leq 1. \end{aligned} \tag{6}$$

Then, we get

$$\begin{aligned} &\sum_{j\geq 0}\sum_{l=-2^j}^{2^j-1}\left|\widehat{\psi}^{(0)}\left(\xi A_0^{-j} B_0^{-l}\right)\right|^2 \\ &= \sum_{j\geq 0}\sum_{l=-2^j}^{2^j-1}\left|\widehat{\psi}_1\left(2^{-2j}\xi_1\right)\right|^2\left|\widehat{\psi}_2\left(2^j\frac{\xi_2}{\xi_1} - l\right)\right|^2 = 1. \end{aligned} \tag{7}$$

Then, $\{\widehat{\psi}^{(0)}(\xi A_0^{-j} B_0^{-l})\}$ form a tiling of the set

$$D_0 = \left\{(\xi_1,\xi_2) \in \widehat{\mathbb{R}}^2 : |\xi_1| \geq \frac{1}{8}, \left|\frac{\xi_2}{\xi_1}\right| \leq 1\right\}. \tag{8}$$

From the condition on the support of $\widehat{\psi}_1$ and $\widehat{\psi}_2$, it is easily deduced that $\widehat{\psi}_{j,l,k}$ have frequency support contained in the set as follows:

$$\operatorname{supp}\widehat{\psi}^{(0)}_{j,l,k} \subset \left\{(\xi_1,\xi_2) : \xi_1 \in \left[-2^{2j-1}, -2^{2j-4}\right] \cup \left[2^{2j-4}, 2^{2j-1}\right], \left|\frac{\xi_2}{\xi_1} + l2^{-2j}\right| \leq 2^{-j}\right\}. \tag{9}$$

Thus, every element in $\psi_{j,l,k}$ is supported on a pair of trapezoids of approximate size $2^{2j} \times 2^j$, oriented along lines of slope $l2^{-j}$[].

For $L^2(D_1)^\vee$, here, D_1 is the vertical cone when the following formula was satisfied:

$$\begin{aligned} D_1 &= \left\{(\xi_1,\xi_2) \in \widehat{\mathbb{R}}^2 : |\xi_2| \geq \frac{1}{8}, \left|\frac{\xi_1}{\xi_2}\right| \leq 1\right\}, \\ A_1 &= \begin{pmatrix} 2 & 0 \\ 0 & 4 \end{pmatrix}, \qquad B_1 = \begin{pmatrix} 1 & 0 \\ 1 & 1 \end{pmatrix}, \\ \widehat{\psi}^{(1)}(\xi) &= \widehat{\psi}^{(1)}(\xi_1,\xi_2) = \widehat{\psi}_1(\xi_2)\,\widehat{\psi}_2\left(\frac{\xi_1}{\xi_2}\right). \end{aligned} \tag{10}$$

Then, collection $\{\psi^{(1)}_{j,l,k}(x) = 2^{3j/2}\psi^{(1)}(B_1^l A_1^j x - k) : j \geq 0, -2^j \leq l \leq 2^j - 1, k \in \mathbb{Z}^2\}$ is a Parseval frame for $L^2(D_1)^\vee$.

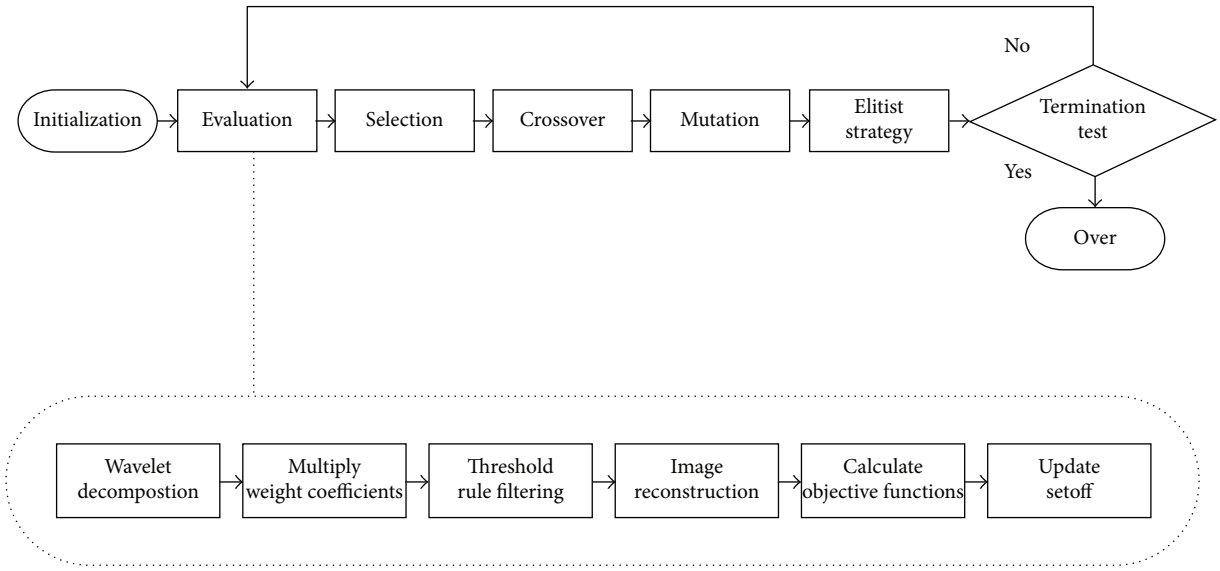

Figure 1: Workflow of proposed algorithm.

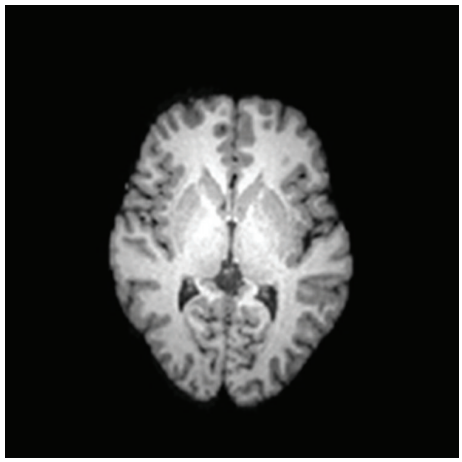

Figure 2: Original MR image.

2.3. Multiobjective Genetic Algorithm (MOGA). Multiobjective genetic algorithm seeks feasible solutions to problems comprising multiple objectives which are often in conflict with each other. A general minimization problem of M objectives can be mathematically stated as $x = [x_1, x_2, \ldots, x_d]$, where d is the dimension of the decision variable space. Consider the following.

Minimize $f(x) = [f_i(x), i = 1, \ldots, m]$ which satisfies

$$\begin{aligned} g_j(x) &\le 0, \quad j = 1, 2, \ldots, J, \\ h_k(x) &= 0, \quad k = 1, 2, \ldots, K, \end{aligned} \tag{11}$$

where $f_i(x)$ is the ith objective function, $g_j(x)$ is the jth inequality constraint, and $h_k(x)$ is the kth equality constraint. The multiobjective optimization problem then reduces to finding an x, such that $f(x)$ is optimized.

3. Proposed Algorithm

3.1. Threshold Rule. Threshold rule is the most important problem in image denoising of transform domain, and the hard-threshold and the soft-threshold approaches are two options. Donoho and Johnstone [16] proposed the following threshold rule:

$$\delta = \sigma\sqrt{2\ln(N)}. \tag{12}$$

Here, N is the pixels number of image, and σ is the noise level.

Research shows that Donoho threshold is the optimal threshold limit not the optimal threshold. With this considered, Donoho and Johnstone [16] proposed an improved threshold rule as follows:

$$\delta_k = \sigma\sqrt{2\ln(N)} * 2^{(k-K)/2}, \quad k = 0, 1, \ldots, K. \tag{13}$$

As many researchers point out [12, 13], (12) did not consider energies of subwavelets in a different direction while being in the same scale, and this imperfection will make coefficients too much stifled.

Considering the variability of image content and Shearlet transformation of multiscale and multidirection characteristics, a novel threshold selection rule is proposed based on Shearlet transform multiscale and multidirection; this rule is the following.

Comprehensively considering complexity of image and the multiscale and multidirection characteristics of Shearlet transform, this paper proposed the following adaptive threshold rule:

$$\begin{aligned} \delta_{k,j} &= \text{Sigmoid}\left(\sigma\sqrt{2\ln(N)} * 2^{(k-K)/2}\right), \quad k = 0, 1, \ldots, K, \\ \text{Sigmoid} &= \frac{1}{1 + e^{-v}}. \end{aligned} \tag{14}$$

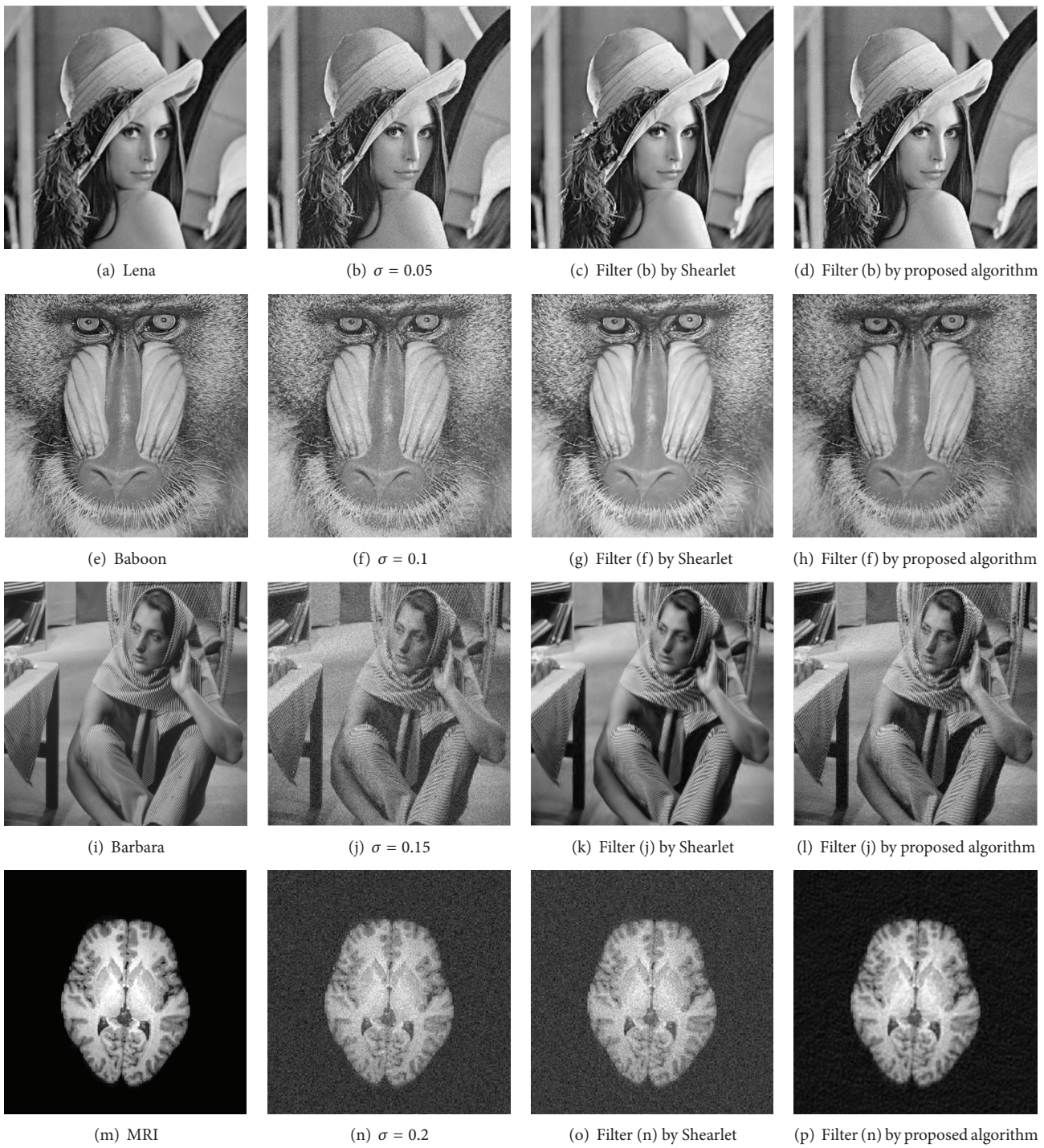

(a) Lena (b) $\sigma = 0.05$ (c) Filter (b) by Shearlet (d) Filter (b) by proposed algorithm

(e) Baboon (f) $\sigma = 0.1$ (g) Filter (f) by Shearlet (h) Filter (f) by proposed algorithm

(i) Barbara (j) $\sigma = 0.15$ (k) Filter (j) by Shearlet (l) Filter (j) by proposed algorithm

(m) MRI (n) $\sigma = 0.2$ (o) Filter (n) by Shearlet (p) Filter (n) by proposed algorithm

Figure 3: Experiment images in different noise levels and different algorithms.

Here, Sigmoid is adopted to build our rules. The Sigmoid curve is a mathematical concept which has been widely used to model the natural life cycle of many things, for its derivative is continuous and with higher accuracy. K is the scale level, and j is the jth direction under the kth scale level.

3.2. Target Function. We build MOGA target function by the signal-to-noise ratio (SNR) and the mean square error (MSE).

Signal-to-noise ratio (SNR) can be defined as

$$\mathrm{SNR} = 10lg\frac{\sum_{i=1}^{M}\sum_{j=1}^{N}A(i,j)^2}{\sum_{i=1}^{M}\sum_{j=1}^{N}\left(A(i,j)-O(i,j)\right)^2}. \quad (15)$$

Here, O is original image with size of $M \times N$ pixels, A is filtered image of noised image, and (i, j) are coordinates of pixels.

Mean square error (MSE) expressed the correlation between images, and it is defined as follows:

$$\mathrm{MSE} = \frac{1}{M \times N} \sum_{i=1}^{M} \sum_{j=1}^{N} \left(A(i,j) - O(i,j)\right)^2. \tag{16}$$

Here, O is original image with size of $M \times N$ pixels, A is filtered image of noised image, and (i, j) are coordinates of pixels.

Our target function is defined as follows:

$$y = \omega_1 \cdot \mathrm{SNR} + \omega_2 \cdot \mathrm{MSE}, \quad 0 \le \omega_1,\ \omega_2 \le 1, \qquad \omega_1 + \omega_2 = 1. \tag{17}$$

Here, ω_1, ω_2 are weight coefficients of SNR and MSE.

3.3. Proposed Model. The most critical problem which lies in our optimal filtering performance study is, under optimization criterion, how to decide coefficients v, $\delta_{k,j}$ considering energy of subwavelets not only in different scale but also in different direction.

Here, we proposed our algorithm which adopts MOGA algorithm to decide coefficients v, $\delta_{k,j}$ of each subwavelet in different scale and direction of Shearlet transform, intending to get optimal filtering performance.

Our algorithm works as follows [17, 18]; see Figure 1.

Step 1 (initialization). Generate an initial population containing N_{pop} strings, where N_{pop} is the number of strings in each population. These strings contain weight coefficients of SNR, MSE, weight coefficients $\delta_{k,j}$ of Shearlet subwavelets, v of S function, and other parameters in MOGA; thus, we need the following.

Step 2 (evaluation).

(1) Use Shearlet transform to decompose target image.

(2) Multiply subwavelets by weight coefficients $\delta_{k,j}$.

(3) Filter subwavelets by threshold rule.

(4) Reconstruct image by filtered subwavelets.

(5) Calculate the values of the objective functions (16) for the generated strings.

(6) Update a tentative setoff Pareto optimal solution.

Step 3 (selection). Calculate the fitness value of each string using the random weights in (3). Select a pair of strings from the current population according to the following selection probability.

Step 4 (crossover). For each selected pair, apply a crossover operation to generate two new strings. N_{pop} new strings are generated by the crossover.

Step 5 (mutation). For each bit value of the strings generated by the crossover, apply a mutation with a prespecified mutation probability.

Table 1: Filtering results for Lena and Barbara.

Image	σ (%)	PSNR	
		Shearlet	Shearlet-MOGA
Lena	10	34.38	35.02
	20	31.79	33.24
	30	29.21	30.21
Barbara	10	33.07	33.07
	20	29.40	29.40
	30	26.31	27.51

Step 6 (elitist strategy). Randomly remove N_{elite} strings from the set of N_{pop} strings generated by previous operations, and replace them with N_{elite} strings randomly selected from tentative set of Pareto optimal solutions.

Step 7 (termination test). If one stopping condition in the following is satisfied, go to Step 8; if not, return to Step 2.

(i) Maximum iterations are exceeded.

(ii) The optimal target value is achieved.

Step 8 (algorithm termination). Exit optimal algorithm.

4. Experimental Results and Analysis

4.1. Evaluation Index. Peak signal-to-noise ratio (PSNR) is defined as

$$\mathrm{PSNR} = 10lg \frac{255^2}{(1/M \times N) \sum_{i=1}^{M} \sum_{j=1}^{N} \left(A(i,j) - O(i,j)\right)^2}. \tag{18}$$

Here, O is original image with size of $M \times N$ pixels, A is filtered image of noised image, and (i, j) are coordinates of pixels.

4.2. Experimental Results. To verify the validity of the algorithm, this paper designed two kinds of experimental methods to verify its effectiveness. One is use of objective data such as PNSR and MSE to objectively analyze its performance; and the other is making us able to obverse filtering performance directly by naked eyes [19–21].

Experiment 1. We did filtering experiments on standard images Lena and Barbara in different noise level and listed results in Table 1. As we have seen from Table 1, PSNR of proposed algorithm (Shearlet-MOGA) is higher than PSNR of classical Shearlet algorithm, and its performance will be better with noise level increased.

Figure 2 is the original MR image we adopted to do experiments. Adding different noise level to Figure 2, we did filtering work by classical Shearlet and proposed algorithm in this paper and showed the statics data of MSE and PSNR as Tables 2 and 3.

In Table 2, the excellent effect of our algorithm is dramatic, shown in and our proposed MSE is smaller than classical Shearlet algorithm. Similar good results were found

Table 2: MSE in different σ (%) and different algorithm to that in Figure 2.

Noise level (%)	5	10	20	30	40	50	60	70	80	90
Classical	25.12	100.4	400.7	905.4	1584	2504	3579	4901	6398	8075
Proposed	10.8	26.52	73.96	147.6	240.9	381	528	705.9	910.7	1132

Table 3: PSNR in different σ (%) and different algorithm to that in Figure 2.

Noise level (%)	5	10	20	30	40	50	60	70	80	90
Classical	34.13	28.11	22.1	18.56	16.13	14.14	12.59	11.23	10.07	9.059
Proposed	40.38	35.93	31.21	28.03	25.77	23.66	22.16	20.82	19.65	18.65

when the same experiment was repeated on PSNR. In Table 3, the PSNR of proposed algorithm is greater than that of classical Shearlet algorithm.

Experiment 2. To evaluate the performance of proposed algorithm by naked eyes directly, several classical images such as Lena, Baboon, Barbara, and MRI are adopted to do filtering work, and all relative images are shown in Figure 3.

Figure 3(a) is the original Lena. Adding 5% Rician noise level to Lena, we get Figure 3(b).

Filtering Figure 3(b) by classical Shearlet algorithm, we got Figure 3(c). Figure 3(d) is the output of the filtering work we did to Figure 3(b) by proposed algorithm.

We did similar experiment to the image of Baboon. Add 10% Rician noise level to Baboon, we get Figure 3(e). Filtering Figure 3(f) by classical Shearlet algorithm, we got Figure 3(g). Figure 3(h) is the output of the filtering work we did to Figure 3(f) by proposed algorithm.

The image of Barbara is also adopted by us to test our algorithm. Figure 3(i) is the original Barbara. Figure 3(j) is Barbara noised by 15% Rician noise level. Filtering Figure 3(j) by classical Shearlet algorithm, we got Figure 3(k). Figure 3(l) is the output of the filtering work we did to Figure 3(j) by proposed algorithm.

At last, we measured our algorithm performance on MRI image. Figure 3(m) is the original MRI. Figure 3(n) is the MRI noised by 20% Rician noise level. Filtering Figure 3(n) by classical Shearlet algorithm, we got Figure 3(o). Figure 3(p) is the output of the filtering work we did to Figure 3(n) by proposed algorithm.

Through simple comparison, we can see that our proposed algorithm could effectively remove the noise from the degraded image of Rician noise with unknown intensity level and protect the image details better at the same time. To MRI image, experiments Paying particular attention data show that our algorithm has excellent performance in background. After strict analysis, we concluded that our algorithm retained the consistent component of low frequency in frequency domain by low-pass filtering, and background of MRI has this nature.

5. Conclusions

In order to eliminate Rician noise and preserve image details as much as possible, this paper proposed a new image-filtering algorithm based on MOGA and classical Shearlet transform. It builds target functions in MOGA by several evaluation methods such as SNR and MSE. It also uses MOGA to find optimal Shearlet wavelet threshold coefficients in a different scale and different orientation. Computer simulations results are given to verify the effectiveness of this algorithm. At last, experiments data show that our algorithm has excellent performance in MRI imaging.

Acknowledgments

Whatever implementation the authors come up with needs to be based on classical Shearlet algorithm, and they cannot execute their work without Professor Labate's earlier work and his open-source code online. The authors would like to thank Professor Labate. The authors would also like to express their thanks to the anonymous reviewers whose comments greatly improved the paper. This paper was funded under a Grant from the National Natural Science Foundation of China (no. 60773172) and a Grant from the Jiangsu Province Natural Science Foundation (BK2008411).

References

[1] H. Gudbjartsson and S. Patz, "The Rician distribution of noisy MRI data," *Magnetic Resonance in Medicine*, vol. 34, no. 6, pp. 910–914, 1995.

[2] E. J. Candes, *Monoscaleridgelets for the Representation of Images with Edges*, Stanford University, 1999.

[3] E. J. Candes and D. L. Donoho, "Curvelets: a surprisingly effective non-adaptive representation for objects with edges," in *Curves and Surfaces Fitting, Saint-Malo 1999*, pp. 105–120, Nashville, Tenn, USA, 2000.

[4] M. N. Do and M. Vetterli, "Contourlets," in *Beyond Wavelets*, G. V. Welland, Ed., Academic Press, 2003.

[5] D. Labate, W. Q. Lim, G. Kutyniok, and G. Weiss, "Sparse multidimensional representation using shearlets," in *Wavelets XI*, vol. 5914 of *Proceedings of SPIE*, pp. 59140U–59140U-9, International Society for Optics and Photonics, August 2005.

[6] S. Yi, D. Labate, G. R. Easley, and H. Krim, "A shearlet approach to edge analysis and detection," *IEEE Transactions on Image Processing*, vol. 18, no. 5, pp. 929–941, 2009.

[7] S. Yi, D. Labate, G. R. Easley, and H. Krim, "Edge detection and processing using shearlets," in *Proceedings of 15th IEEE International Conference on Image Processing (ICIP '08)*, pp. 1148–1151, IEEE, October 2008.

[8] G. R. Easley, D. Labate, and F. Colonna, "Shearlet-based total variation diffusion for denoising," *IEEE Transactions on Image Processing*, vol. 18, no. 2, pp. 260–268, 2009.

[9] S. Yi, D. Labate, G. R. Easley, and H. Krim, "A shearlet approach to edge analysis and detection," *IEEE Transactions on Image Processing*, vol. 18, no. 5, pp. 929–941, 2009.

[10] G. R. Easley, D. Labate, and W.-Q. Lim, "Optimally sparse image representations using shearlets," in *Proceedings of the 40th Asilomar Conference on Signals, Systems, and Computers (ACSSC '06)*, pp. 974–978, October-November 2006.

[11] X. Chen, C. Deng, and S. Wang, "Shearlet-based adaptive shrinkage threshold for image denoising," in *Proceedings of the 1st International Conference on E-Business and E-Government (ICEE '10)*, pp. 1616–1619, May 2010.

[12] H. Sun and J. Zhao, "Shearlet threshold denoising method based on two sub-swarm exchange particle swarm optimization," in *Proceedings of IEEE International Conference on Granular Computing (GrC '10)*, pp. 449–452, IEEE, August 2010.

[13] A. Firouzmanesh and P. Boulanger, "Image De-blurring using shearlets," in *Proceedings of the 9th Conference on Computer and Robot Vision (CRV '12)*, pp. 167–173, May 2012.

[14] Q. Guo, S. Yu, X. Chen, C. Liu, and W. Wei, "Shearlet-based image denoising using bivariate shrinkage with intra-band and opposite orientation dependencies," in *Proceedings of the International Joint Conference on Computational Sciences and Optimization (CSO '09)*, vol. 1, pp. 863–866, IEEE, April 2009.

[15] T. Sun and Y. Neuvo, "Detail-preserving median based filters in image processing," *Pattern Recognition Letters*, vol. 15, no. 4, pp. 341–347, 1994.

[16] D. L. Donoho and I. M. Johnstone, "Adapting to unknowns-moothness via wavelet shrinkage," *Journal of the American Statistical Association*, vol. 12, no. 90, pp. 1200–1224., 1995.

[17] T. Murata and H. Ishibuchi, "MOGA: multi-objective genetic algorithms," in *Proceedings of IEEE International Conference on Evolutionary Computation*, vol. 1, pp. 289–294, IEEE, November-December 1995.

[18] K. Deb, "Multi-objective genetic algorithms: problem difficulties and construction of test problems," *Evolutionary Computation*, vol. 7, no. 3, pp. 205–230, 1999.

[19] T. Li and X. Ye, "Improved stability criteria of neural networks with time-varying delays: an augmented LKF approach," *Neurocomputing*, vol. 73, no. 4–6, pp. 1038–1047, 2010.

[20] J. Xu, Y.-Y. Cao, D. Pi, and Y. Sun, "An estimation of the domain of attraction for recurrent neural networks with time-varying delays," *Neurocomputing*, vol. 71, no. 7–9, pp. 1566–1577, 2008.

[21] M. Xia, J. Fang, Y. Tang, and Z. Wang, "Dynamic depression control of chaotic neural networks for associative memory," *Neurocomputing*, vol. 73, no. 4–6, pp. 776–783, 2010.